

## COMMON SHOT GATHER MODELING AND INVERSION

*Allan Snyder*

### *Abstract*

The monochromatic  $45^\circ$  equation and the phase shift method are used to generate and invert common shot gathers (CSG's). The modeling algorithm uses the basic principle  $U = cD$ , where  $U$  is the upgoing wave,  $c$  is the reflection coefficient and  $D$  is the downgoing wave. The basic idea of the inversion process is to find those points in space where the up- and downgoing waves are time-coincident, which is where reflectors exist. This method has an advantage over the standard industrial migration procedure in that it handles lateral velocity variation and steeply dipping beds, which invalidate the standard assumption in industry that a zero-offset section is identical to a CDP stack.

### *Introduction*

The standard industrial migration process is to do a CDP stack and then migrate the stacked section, assuming that it is a zero-offset section. For areas without significant lateral velocity variation and with relatively flat beds, this is a good approximation, but otherwise this assumption breaks down (see Figures 1 and 2). The CSG inversion technique to be discussed in this paper can handle significant lateral velocity variation and steep dips, which are often found in geologically disturbed areas.

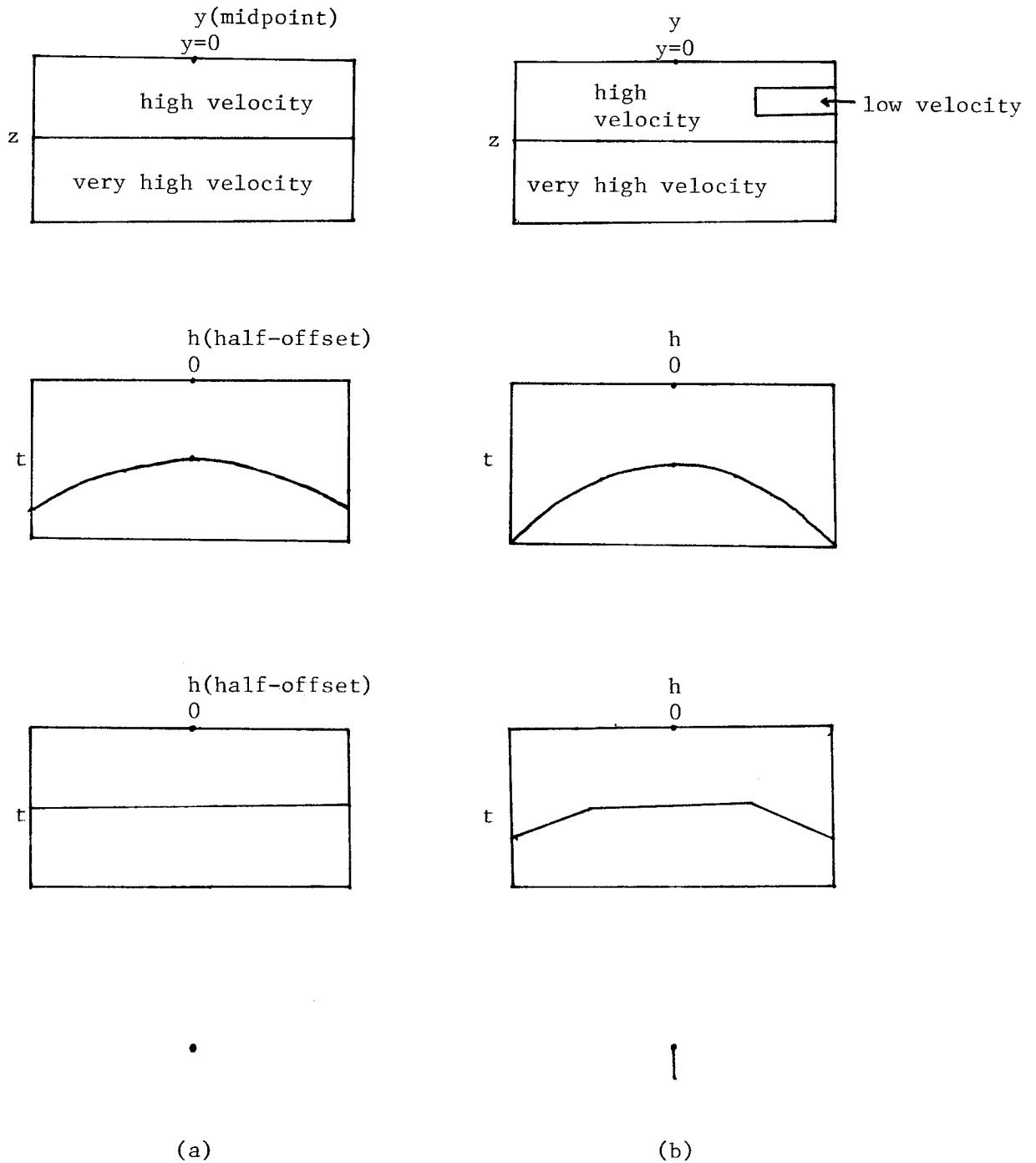


FIGURE 1.--(a) Velocity model, common midpoint gather, common midpoint gather with NMO applied and final stacked trace for an area with stratified media. A zero offset section would be identical to this. (b) The same for an area with a low velocity zone, with the high velocity used for NMO once again. A zero offset section for this geometry would give the same result as in (a), which is not what we get here, thus demonstrating the non-equivalence of a zero-offset section and a CDP stack with lateral velocity variation.

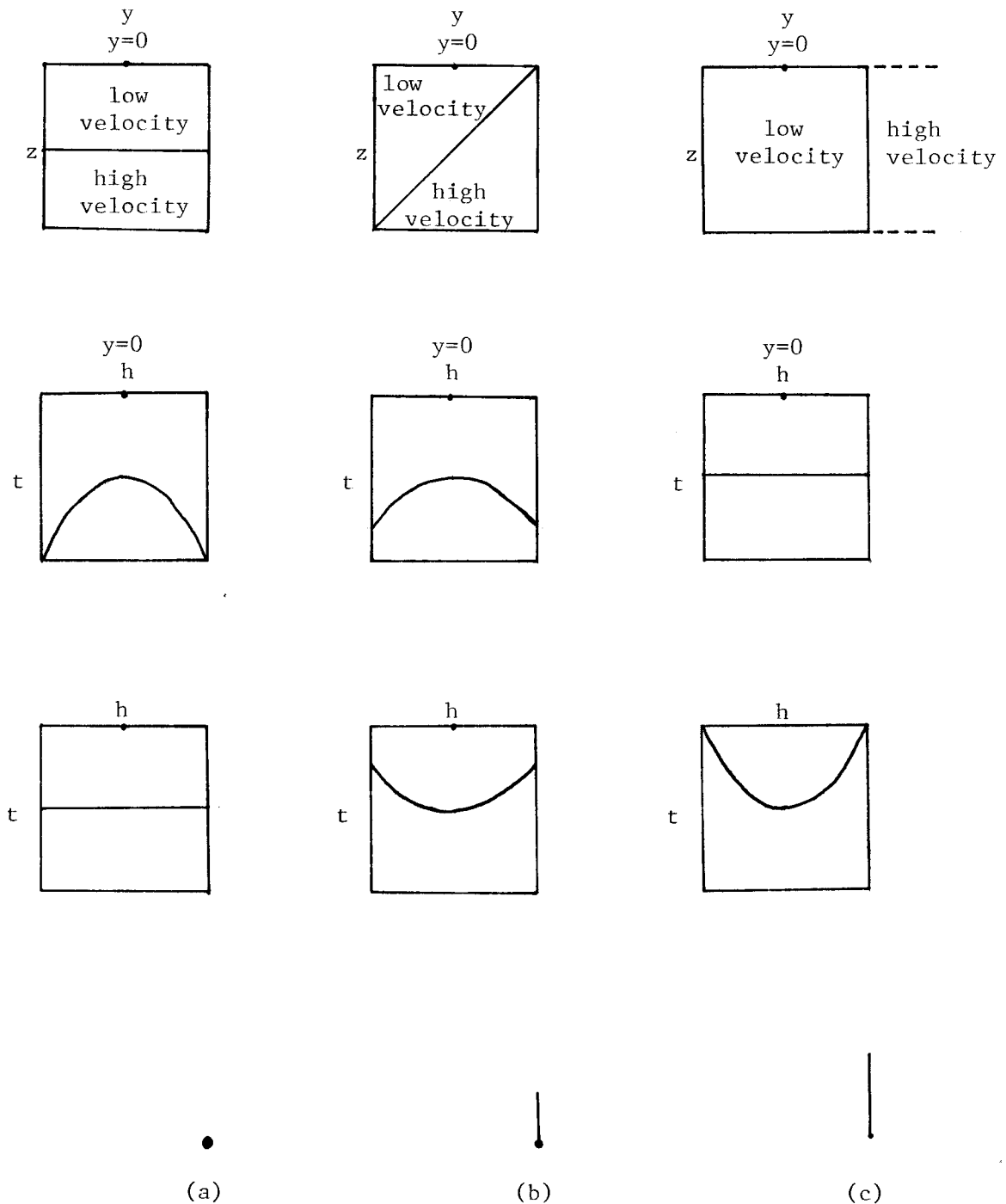


FIGURE 2.--(a) Velocity model, common midpoint gather, common midpoint gather with NMO applied and final stacked trace for a flat bed. A zero-offset section would be identical to this. (b) The same for a  $45^\circ$  dipping bed, with the low velocity used for NMO once again. A zero-offset section would give a point in the middle of the tail of the bottom figure, which is not what we get. (c) The same for a vertical bed, with the same NMO. A zero-offset section would give a point as in (a). These demonstrate the non-equivalence of a CDP stack and a zero-offset section for dipping beds.

*Modeling*

We start with  $c(x,z)$ , the reflection coefficients as a function of lateral position  $x$  and vertical position  $z$ ,  $v(x,z)$ , the velocity, and an initial downgoing wave  $D(x,z=0,\omega)$ , where  $\omega$  is angular frequency, which is non-zero wherever we choose to fire off our shots, and has a magnitude proportional to the strength of each shot. It is independent of  $\omega$  if we assume a delta function source. Then we construct  $D(x,z,\omega)$  by downward continuing each frequency through the velocity structure of the model using the following two equations, which represent the monochromatic 45° equation downward continuation method (Kjartansson, SEP-15, pp. 1-20).

$$\frac{i v(x,z)}{2\omega} D_{\text{xxz}} + D_{\text{xx}} + \frac{2i\omega}{v(x,z)} D_z = 0 \quad (1)$$

$$D_z = \frac{i\omega}{v(x,z)} D$$

where the subscripts indicate partial derivatives. There are ways of getting higher angular accuracy and stability with any amount of lateral velocity variation (Godfrey and Jacobs, this report), but for most practical purposes Kjartansson's method is sufficient.

With only depth-variable or constant velocity we use the phase-shift method (Gazdag, 1978), also called the telescope equation, for downward continuation. The following extrapolation equation is used:

$$D(k_x, z+\Delta z, \omega) = D(k_x, z, \omega) e^{i\Delta z \{ [\omega^2/v^2(z)] - k_x^2 \}^{1/2}}$$

Next we use the standard zero offset section approach and start with  $U(x, z_{\text{max}}, \omega)$ , the upgoing wave at the bottom of the grid, equal to zero. We then upward continue it through the velocity structure of the model to the surface, using the same algorithm as with downward continuation, with sources wherever the reflection coefficients are not zero. The difference between this scheme and the zero offset case is that the sources are  $cD$ , not  $c$  as with zero offset. We record  $U(x, z=0, \omega)$  and then inverse Fourier transform to get  $U(x, z=0, t)$ , which is a CSG.

Note that the shot does not have to be in the center of the grid and in fact can be off the grid completely in order to simulate marine

data. To simulate a marine CSG, we can compute  $D$  for the grid spanned by the shot and geophones, but then only calculate  $U$  for the grid spanned by the geophones. It turns out that the same thing can be done with inversion.

### *Inversion*

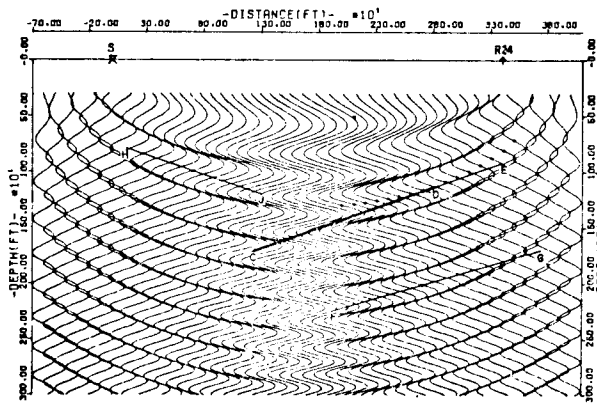
Inversion proceeds in a similar way. We need  $D(x,z,\omega)$ , which can be computed just as with modeling, along with  $v(x,z)$  and  $U(x,z=0,t)$ , the recorded CSG. We Fourier transform  $U(x,z=0,t)$  to get  $U(x,z=0,\omega)$  and then downward continue it one  $z$ -step with the  $45^\circ$  equation or the phase shift method once again to get  $U(x,\Delta z,\omega)$ .

Now we need to derive some relations for  $c$  in terms of  $U$  and  $D$ . We use the imaging principle, "Reflectors exist in the earth at places where the onset of the downgoing wave is time-coincident with an upcoming wave" (Claerbout, 1976). For a monochromatic source, the up- and downgoing waves will be phase at the reflector. However, there will also be many other places where the waves will be in phase. To remove this ambiguity, the true image is obtained by superimposing the images produced by many different monochromatic sources. Figure 3 from Peterson and Walter (1977), nicely illustrates this principle. Thus we are using the following equation for  $c$  (Claerbout, 1971):

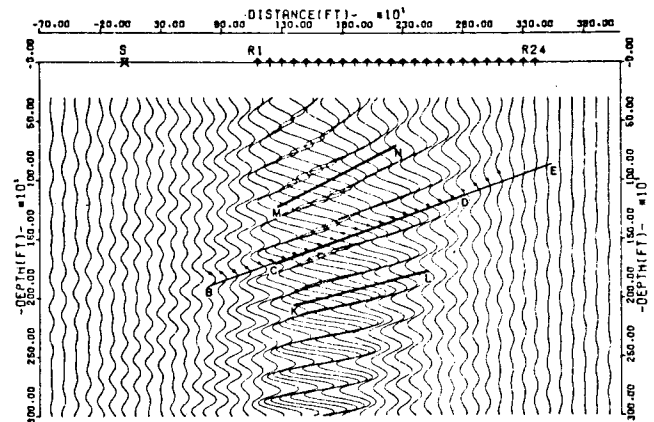
$$c(x,\Delta z) \approx \frac{U(x,\Delta z,\omega)}{D(x,\Delta z,\omega)} \quad (2)$$

From this we can derive four almost equivalent expressions:

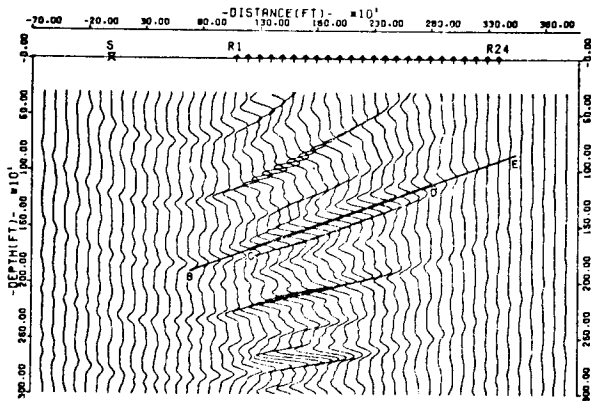
$$c(x,\Delta z) \sim \left[ \begin{array}{l} \sum_{\omega} \frac{U(x,\Delta z,\omega)}{D(x,z,\omega) + \epsilon} \quad (3) \\ \sum_{\omega} \frac{U(x,\Delta z,\omega) D^*(x,\Delta z,\omega)}{D(x,\Delta z,\omega) D^*(x,\Delta z,\omega) + \epsilon} \quad (4) \\ \sum_{\omega} U(x,\Delta z,\omega) D^*(x,\Delta z,\omega) \quad (5) \\ \frac{\sum_{\omega} U(x,\Delta z,\omega) D^*(x,\Delta z,\omega)}{\sum_{\omega} D(x,\Delta z,\omega) D^*(x,\Delta z,\omega)} \quad (6) \end{array} \right.$$



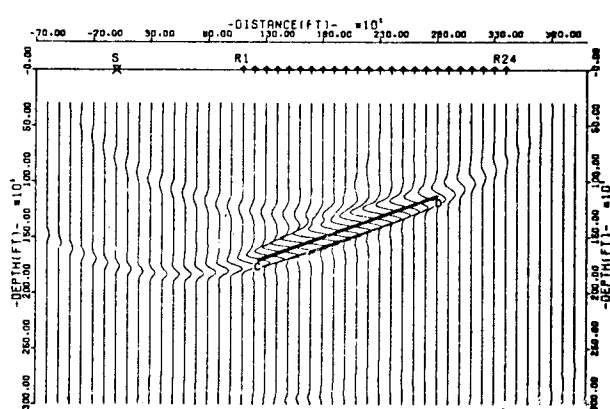
(a)



(b)



(c)



(d)

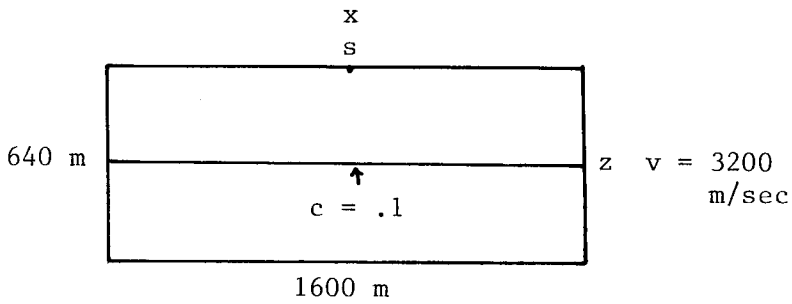
FIGURE 3. (from Peterson and Walter, 1977)--Holographic imaging of a truncated bed using a single source and 24 receivers. (a) Reconstruction of the reflecting subsurface using a single frequency and only one geophone. The location of the reflector is unrecognizable. (b) Lateral resolution is increased by superimposing the reconstructions from all 24 geophones. (c) Vertical resolution is increased by superimposing six different frequency reconstructions like (b). (d) Superposition of 26 frequencies using all geophones. The location of the bed is now easily recognized.

where  $*$  indicates complex conjugate and  $\epsilon$  is a small number added in to cure a zero-divide problem. The idea here is to crosscorrelate the downgoing wave at the travelttime that it takes to get to the reflector with the upcoming wave at zero travelttime. These expressions reduce to the zero-offset case  $[c(x,\Delta z) = \sum_{\omega} U(x,\Delta z,\omega)]$  if  $D = 1$  and  $\epsilon = 0$ .  $D^*$  is introduced to make real numbers out of the denominators and hence reduce them to scaling factors only. Equations (4), (5) and (6) have been implemented. We can get Equation (5) from (4) by ignoring the denominator of (4), which means that the results of (5) must be exponentially gained to get true amplitudes out of them. Equation (6) has problems with noise caused by division by  $\sum_{\omega} D D^*$ , which varies quite a bit. Equation (4) has the same problem with  $D D^*$  if  $\epsilon$  is very small, but if  $\epsilon$  is large it dominates  $D D^*$  and then (4) essentially behaves like (5). Deciding what value to use for  $\epsilon$  is troublesome, however. See Figures 4 and 5 for a comparison of the  $c$  estimators.

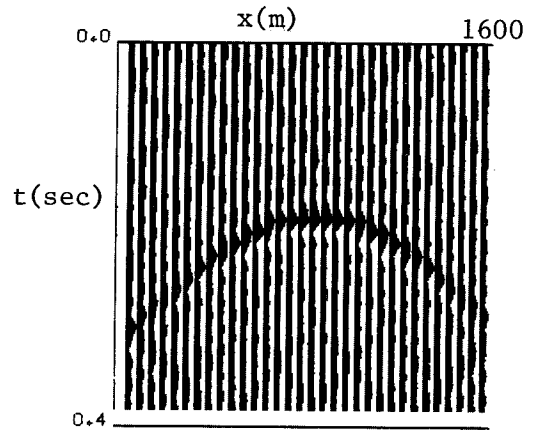
Now that we have estimated  $c$  at this  $z$ -level, we then downward continue to the next  $z$ -level and compute  $c$  once again, and continue in this manner all the way to the bottom of the grid. We then have  $c(x,z)$  for the grid spanned by the horizontal extent of the geophones plus the width of the area that is zero-padded (see Figure 8) and the maximum depth we downward continue to. The grids for adjacent inverted CSG's overlap each other considerably and so we can stack the overlapping results in some way to get the final  $c$ 's for the whole line. The result is a migrated depth section such as that obtained in normal processing by collection into common midpoint gathers, normal moveout (NMO), stacking, time migration and then finally time-to-depth conversion. The depth section can be converted back to time by the usual method if so desired by the interpreter, or the CSG inversion scheme can be modified to yield migrated time sections (Lynn, SEP-14, pp. 87-94).

### *Problems*

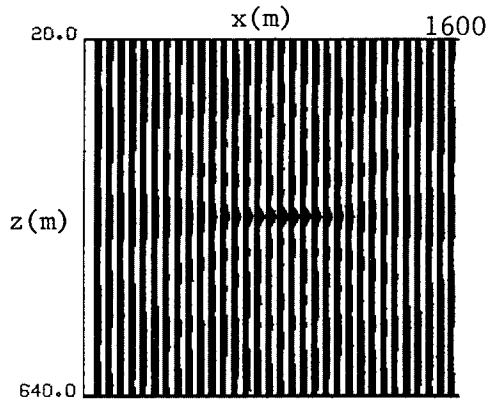
The first problem is the shot waveform. This problem is common to all migration methods and so we usually do deconvolution before inversion and hope that we have reduced the shot waveform to something resembling a delta function. It is possible to include the estimated shot waveform with the downgoing wave and try to process non-deconvolved data but since we never have a good estimate of the shot waveform this method is doomed to failure. The other possibility is to deconvolve after



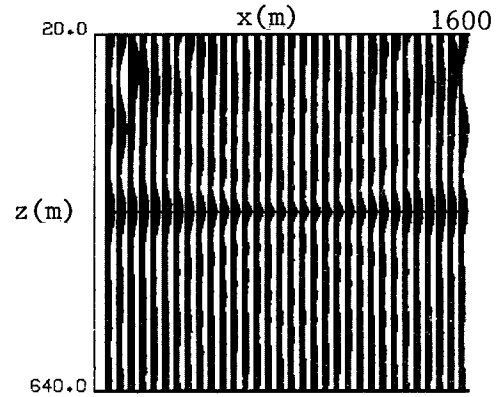
(a)



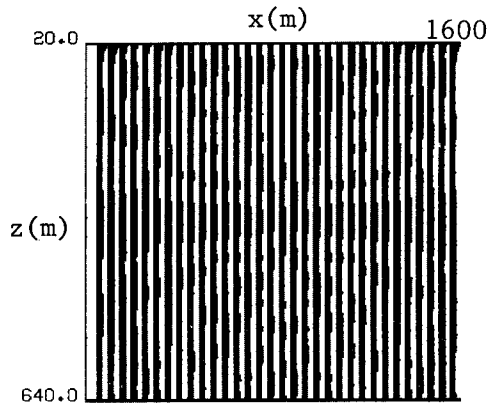
(b)



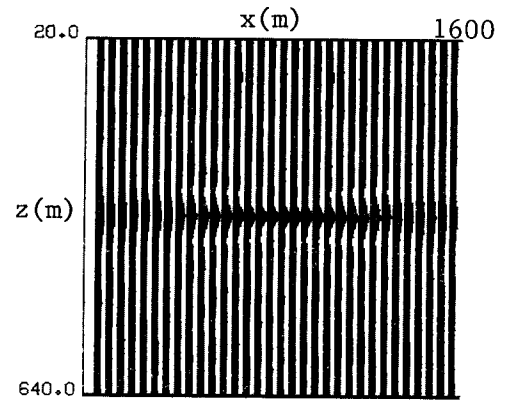
(c)



(d)



(e)



(f)

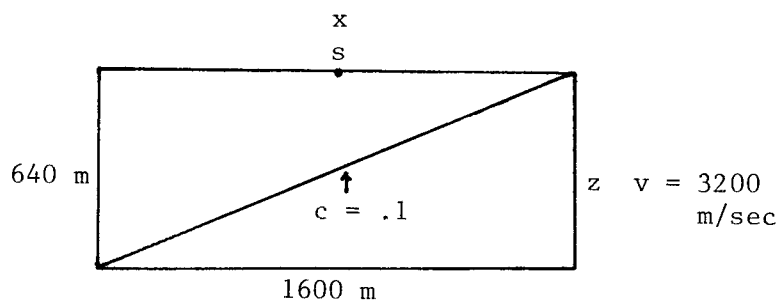
FIGURE 4.--

(a) Model.

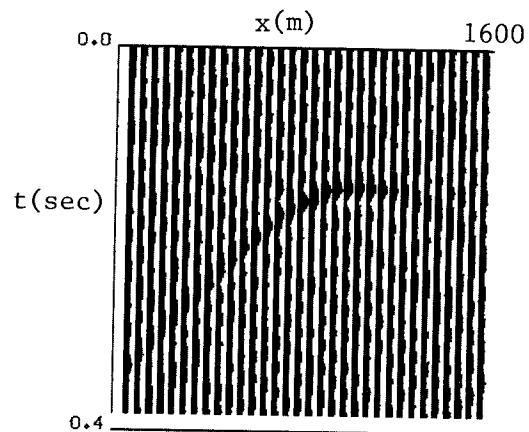
(b) CSG generated from (a) using the phase shift method.

(c) Inversion of (b) using the phase shift method and  $\sum_{\omega} UD^*$ .(d) Inversion of (b) using the phase shift method and  $\sum_{\omega} UD^*/\sum_{\omega} DD^*$ .(e) Inversion of (b) using the phase shift method and  $\sum_{\omega} (UD^*/DD^*)$ .(f) Inversion of (b) using the phase shift method and  $\sum_{\omega} [UD^*/(DD^* + .01)]$ . This gives the best results.

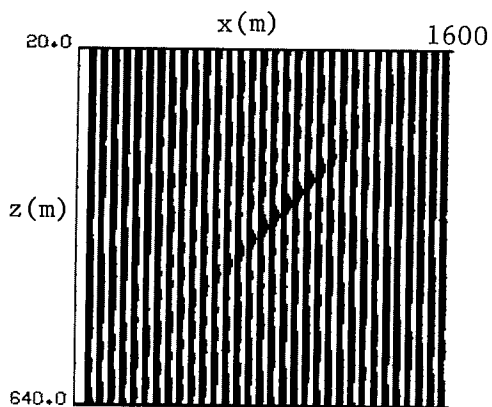




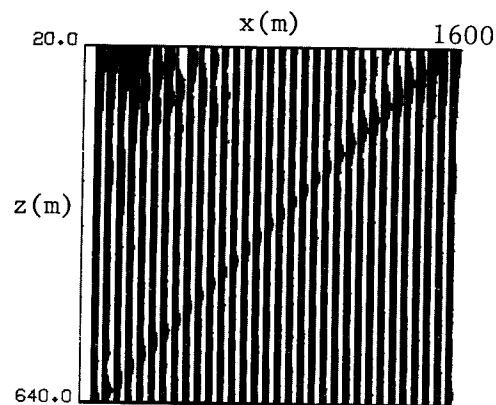
(a)



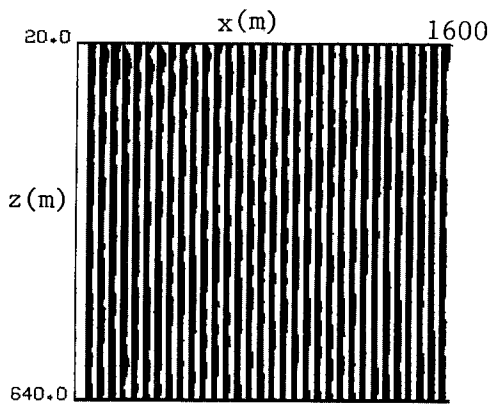
(b)



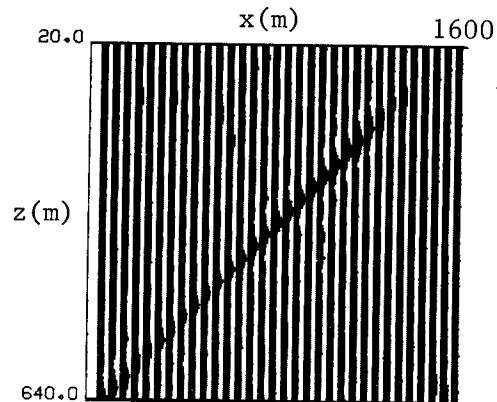
(c)



(d)



(e)



(f)

FIGURE 5.--

(a) Model.

(b) CSG generated from (a) using the phase shift method.

(c) Inversion of (b) using the phase shift method and  $\sum \omega UD^*$ .

(d) Inversion of (b) using the phase shift method and  $\sum \omega UD^* / \sum \omega DD^*$ .

(e) Inversion of (b) using the phase shift method and  $\sum \omega (UD^*/DD^*)$ . This has the same problem as (d).

(f) Inversion of (b) using the phase shift method and  $\sum \omega [UD^*/(DD^* + .01)]$ . This gives the best results once again.

inversion, as we can invert the CSG assuming a delta function shot waveform, which just gives an inverted section with the shot waveform still there.

The next problem is velocity estimation. We must know the velocity in order to carry out the inversion. This is a problem with all migration schemes, but with this one it is especially acute since this method is useful only where there is significant lateral velocity variation, but no one has come up with a good velocity estimation method to handle lateral velocity variation. CSG inversion is quite sensitive to velocity errors (see Figure 6), which is useful in suppressing multiples (see below) and in velocity estimation (see page 75), but causes trouble when we do not know the velocity very well. Work is currently being done on what appears to be an excellent estimation procedure for lateral velocity variation, however (Lynn, SEP-14, pp. 95-118, and SEP-15, pp. 39-56).

Another problem which there is no way around is that interpreters like to have an unmigrated time section as an intermediate product in the data processing procedure, which CDP stacking gives but CSG inversion does not.

It might appear that CDP stacking has an advantage over CSG inversion with regard to signal-to-noise ratio and multiples, but this is not true. Multiples will be migrated with the wrong velocities and will be dispersed considerably in the inverted sections (see Figure 7) due to the velocity sensitivity of CSG inversion, and upon stacking most of the noise still present in each inverted CSG will tend to cancel out compared to the coherent events, which will add together, just as with a CDP stack. In fact, as demonstrated in Figures 1 and 2, a CDP stack will be noisier than a CSG inversion if there is lateral velocity variation or dip.

Cost is a major problem with this scheme. The standard industrial procedure of gathering into common midpoint gathers, NMO, stacking, time migration and time-to-depth conversion is very cheap compared to the cost of migrating all of the CSG's and then stacking them. It is hoped that the improvement in accuracy will more than offset the increased cost. With oil costs rising in general due to its scarcity, increased processing costs may be less of a factor in the future. Note that there is no advantage to CSG inversion in areas of stratified media and no dip, where conventional processing will still be the best choice, since it is just as accurate and much cheaper. Even if CSG inversion proves to be no more accurate than conventional techniques, if it turns out to be useful with multiples it may be worth the extra cost in multiple-prone areas (see page 80).

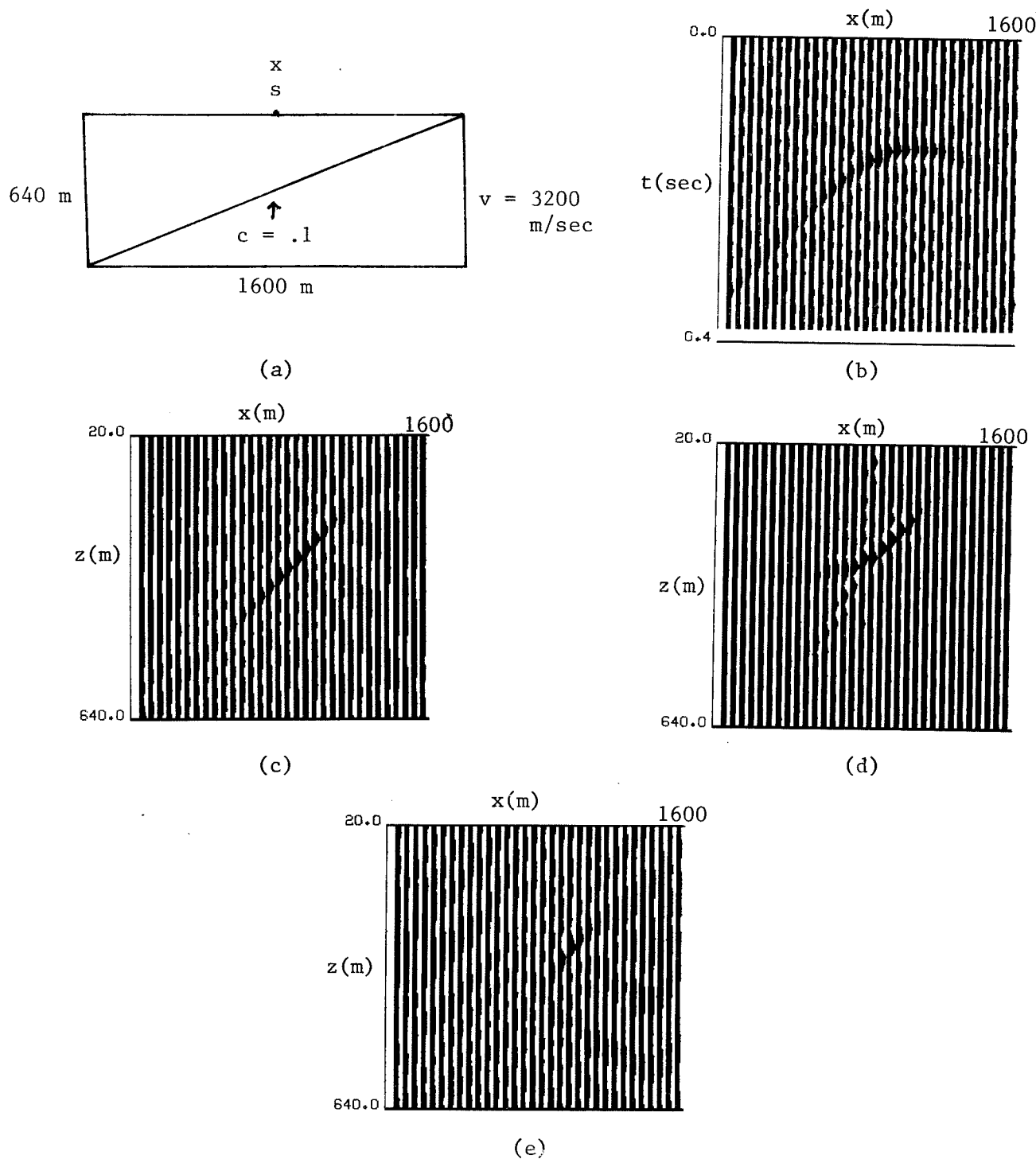
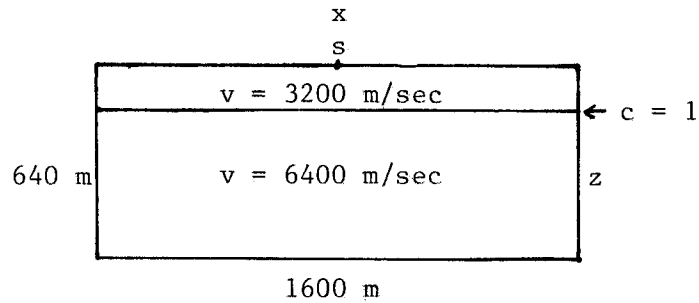
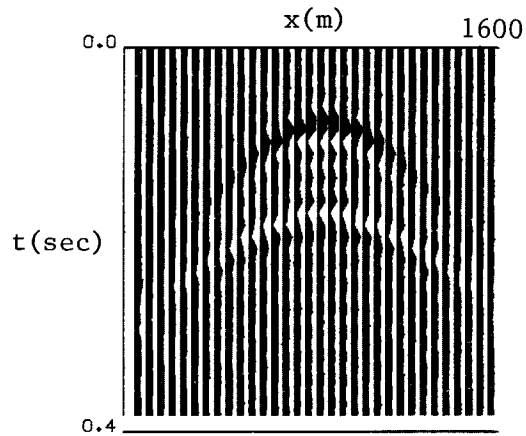


FIGURE 6.--

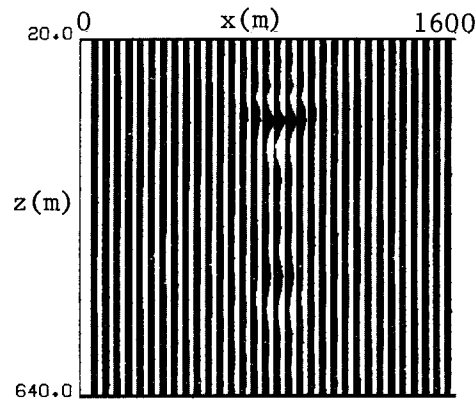
- (a) Model.
- (b) CSG generated from (a) using the phase shift method.
- (c) Inversion of (b) using the phase shift method,  $\sum \omega UD^*$  and the right velocity.
- (d) Inversion of (b) using the phase shift method,  $\sum \omega UD^*$  and a velocity of 2800 m/sec. Note how much more coherent (c) is. This shows the sensitivity of this method.
- (e) Inversion of (b) using the phase shift method,  $\sum \omega UD^*$  and a velocity of 3600 m/sec. This gives results similar to (d).



(a)



(b)



(c)

FIGURE 7.--(a) Model. (b) CSG produced from (a) using the phase shift method and including the first multiple. (c) Attempted inversion of (b) using the phase shift method and  $\sum \omega UD^*$ . The top event is the primary, which is clearly focused better than the multiple. This is because the inversion program thinks the multiple has a velocity of 6400 m/sec, when it only has a velocity of 3200 m/sec, and thus it is not migrated properly, which is what we want. CDP stacking does the same sort of thing.

The last and perhaps most important problem is end effects. Usually we will only have about 48 traces to work with, compared to about 1000 time points, and so there will be a shortage of traces to work with. It is possible for reflectors off the end or the inside of the geophone spread to reflect energy onto the geophones, not to mention crossdip. See Figure 8 for a way to deal with this. Figure 9 shows the various field geometries and how they are related to end effects.

A way of getting around the end effects problem, though it does remove the shot space aliasing advantage of CSG inversion (see below) is to slant stack each of the CSG's (Schultz, SEP-9). This consists of applying linear moveout to a CSG, with the slope of the correction depending on  $p$ , the ray parameter, and then stacking all of the traces together. Different  $p$  values enhance different parts of the gather, depending on the slope of the data on the gather. This will change the lateral coordinate to midpoint rather than offset, thus reducing the end effect problem considerably, since there are many more midpoints than offsets. Each section could be inverted by using a slant plane wave as the initial condition instead of a single shot, and then otherwise following the same procedure as before. This could be done for several different  $p$  values to enhance different areas of the section and then, if desired, all of the sections could be stacked together. Thus, instead of inverting 1000 CSG's, about 10 sections with different  $p$  values would be inverted, which would be cheaper by a factor of about 10, since we would invert 10 1000-trace sections instead of 1000 96-trace sections (allowing for zero padding of 24 traces on each side). Slant stacks have the disadvantage, however, of introducing aliasing and often destroying information in the CSG's when stacking, much as a CDP stack does.

#### *Comparison with other methods*

So far CSG inversion has only been compared to the standard zero offset industrial migration process. There are four other migration schemes that also claim to have advantages over the conventional method. These are constant offset section migration (also called migration before stack), Devilish, shot-geophone migration, and slant midpoint migration.

One advantage that CSG inversion has over all of the above methods is that it has no problem with shot space aliasing. All of the other schemes must have closely spaced shot points in order to get good results, while CSG inversion works with one CSG at a time, and thus it does not matter how

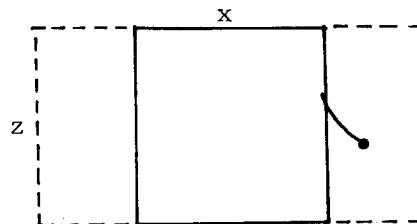
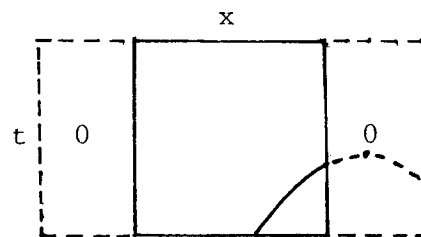
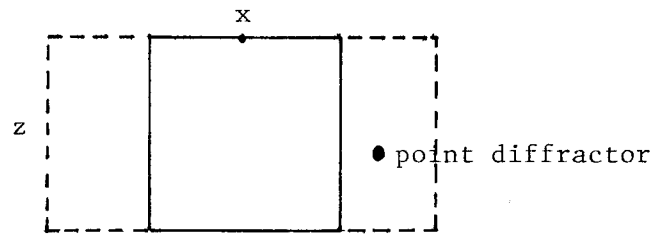


FIGURE 8.--Model, CSG and inverted CSG for a point diffractor off the grid. This illustrates how zero padding on each end of the grid allows reflectors off the grid to be imaged somewhat. Otherwise the energy would be absorbed or reflected off the boundaries, which implies that it is lost or incorrectly positioned. The same thing can be done when the near traces are missing (see Figure 9). The amount of zero padding needed is an open question right now and will depend on the grid size used.

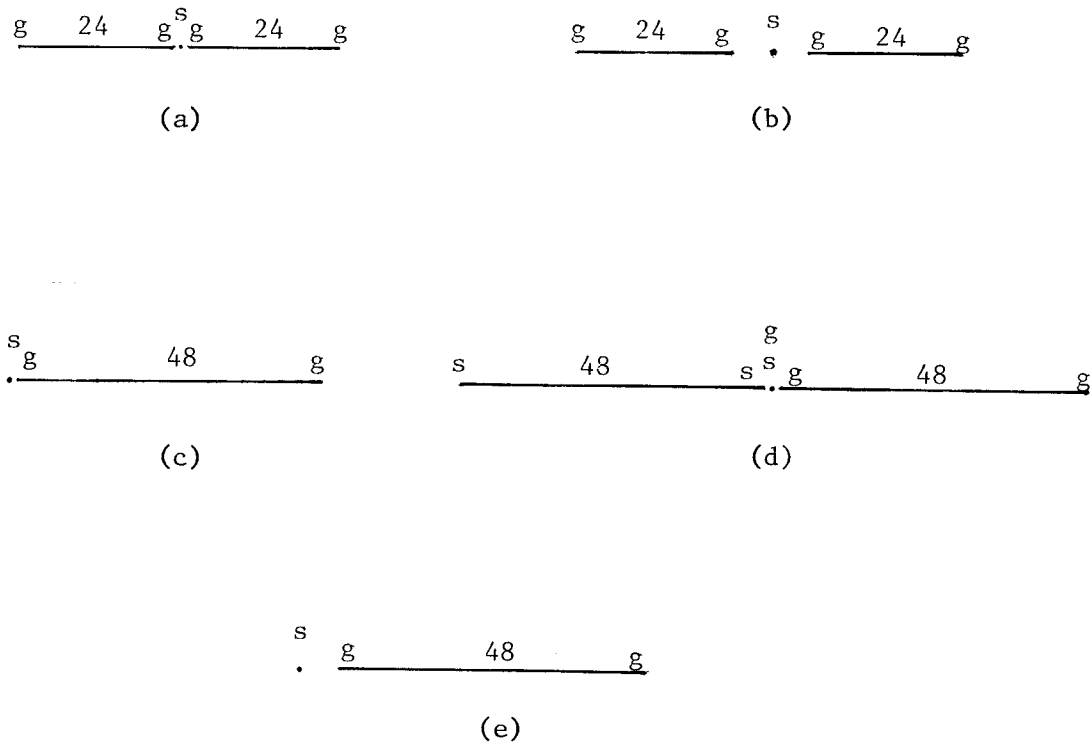


FIGURE 9.--(a) Split-spread field geometry with the near offsets small. The zero-offset trace can be extrapolated accurately and thus there is no end effect problem around zero offset. We can work with 48 contiguous traces. This is the most common land shooting arrangement. (b) Same geometry with large near offsets. The small offset traces cannot be extrapolated accurately, which causes end effect problems around zero offset and allows us to work with only 24 contiguous traces. An alternate way of handling this would be to migrate the gathers on the left and right of the shot separately, but this would be worse, as we would then have to zero-pad a lot to the left or right of the shot to image diffractors there. (c) and (d) Marine geometry with a small near offset. Using reciprocity we can couple this data with a common geophone gather consisting of a geophone at the shot location and an array of shots that is the mirror image of the original CSG. Now we can extrapolate the zero-offset trace and then work with 96 contiguous traces, thus reducing the end effects problem considerably. This cannot be done with a split-spread arrangement. (e) Marine geometry with a large near offset. Reciprocity could be invoked here, too, and would help the zero-padding problem near zero offset, since diffractors far to the left of the shot could be imaged in the reciprocal common geophone gather without doing a lot of zero-padding.

close together the shots are. Hence, in areas of rugged topography where getting closely spaced shots is hard or impossible, CSG inversion may be the way to go, especially since such areas usually have significant lateral velocity variation. Multiplicity is still desired whenever it is practical, however, as discussed previously. Field setups might be geared towards fewer shots but longer spreads and/or more closely spaced geophones. This would be cheaper than conventional techniques, since laying geophones is cheaper than firing shots, and it would also cut down on the end effects problem.

Constant offset section migration would cost half as much as CSG inversion due to no zero padding and would not have nearly the end effect problem due to using midpoint rather than offset as the lateral coordinate, but unfortunately no one has been able to come up with a good way of doing it as yet when there is significant lateral velocity variation.

Devilish, pioneered by Digicon (Judson et al, 1978), maps non-zero-offset data into zero offset and then stacking and migration is done as usual. The idea is to change the steeply dipping data in non-zero-offset data so that it will stack using a flat dip velocity function. It is relatively cheap compared to CSG migration, since converting one type of hyperbola into another takes much less computer time than collapsing a hyperbola. It has the additional advantage of generating an unmigrated time section as an intermediate product, which is helpful to interpreters. Unfortunately, Digicon has not disclosed how it does Devilish, though attempts are being made to figure it out (Deregowski and Rocca, this report, and Claerbout and Yilmaz, also this report). Devilish is designed to handle steep dips; however, it is not designed for lateral velocity variation.

Shot-geophone (s-g) migration involves downward continuing the shots and geophones into the earth and picking off the migrated depth section at zero travelttime and zero offset for each z-level (Lynn, SEP-14, pages 5-12). We must work with all of the recorded data at once and alternately doward continue CSG's and common geophone gathers. This can be done using one  $\omega$  at a time with Kjartansson's method, and it turns out that there is about as much data handling as with CSG inversion, since all of the data for one  $\omega$  will normally fit in an array processor, thus eliminating the reordering from CSG's to common geophone gathers problem. S-g migration's end effect problem is similar to CSG inversion's



except that less zero-padding is needed for the far offsets, since here we only downward-continue one z-step at a time versus all the way with CSG inversion. This method will handle lateral velocity variation, and so it will be interesting to see how it compares with CSG inversion, as work is being done on it now.

Slant midpoint migration involves slant stacks of common midpoint gathers (Ottolini, SEP-14, pp. 37-58). Then every stacked section, each made with a different  $p$  value, is migrated using a Stolt-type algorithm. The cost is slightly less than the CSG slant stacking method described on page 71 due to the greater speed of frequency domain methods. It also has the advantage of producing an unmigrated time section as an intermediate product. Besides the aforementioned aliasing problem, slant midpoint migration has the limitation of only being designed for depth-variable velocity. It has been tested against Devilish and conventional processing and has been found to perform better than the conventional method but not as well as Devilish (Ottolini, 1978).

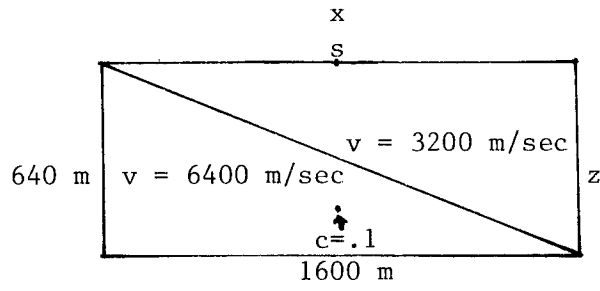
### *Examples*

Figures 10-13 show some examples of CSG modeling and inversion with the  $45^{\circ}$  equation and lateral velocity variation. Note that so far the inversion technique has only been tested on synthetic data generated by the inversion scheme run backward. This really does not prove anything, and so the next step is to try it on synthetic data generated by other means from more complex models. Eventually real data will be used.

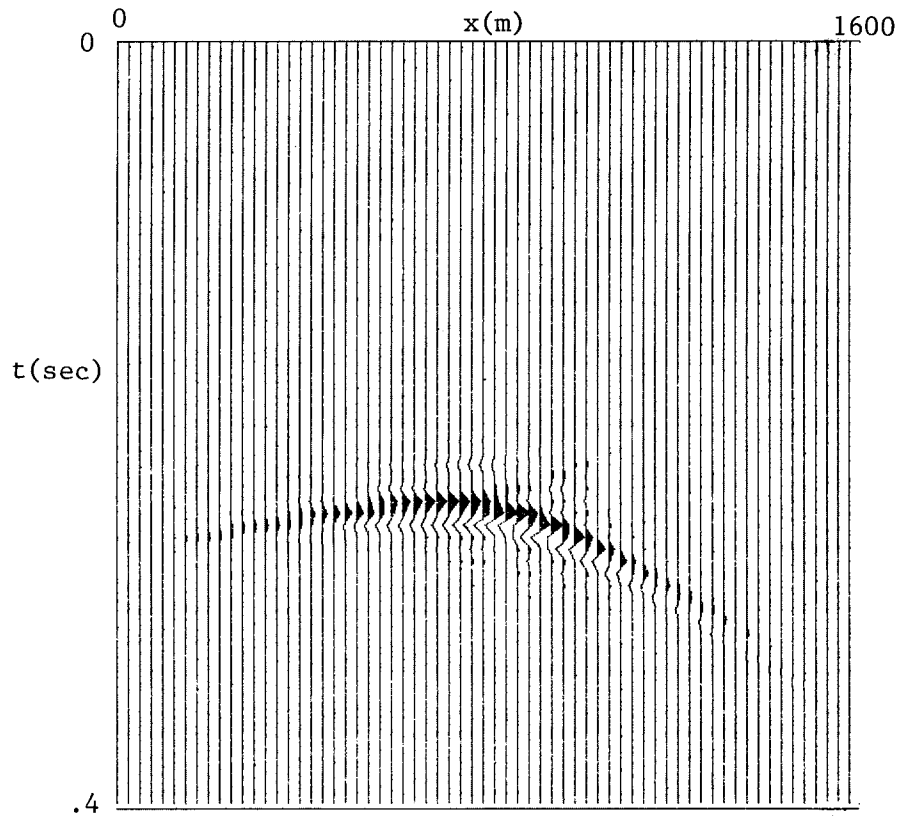
### *Future directions*

A possible application of CSG inversion is with velocity estimation. Laterally coherent events should be continuous when correlated across adjacent inverted CSG's, and if they are not, it is a sure sign that the lateral velocity variation in the area has not been estimated correctly. Thus, inversion with different velocity functions can serve as a method for getting the right velocity function in an area with lateral velocity variation. However, some means of estimating velocity beforehand must be used.

The other potential application is in the suppression of multiple reflections. CSG modeling offers a way of modeling them very accurately, since we simply use the negative of the upcoming wave at the surface as the initial condition for the downgoing wave in order to generate the



(a)



(b)

FIGURE 10.--(a) Model. (b) CSG generated from (a).

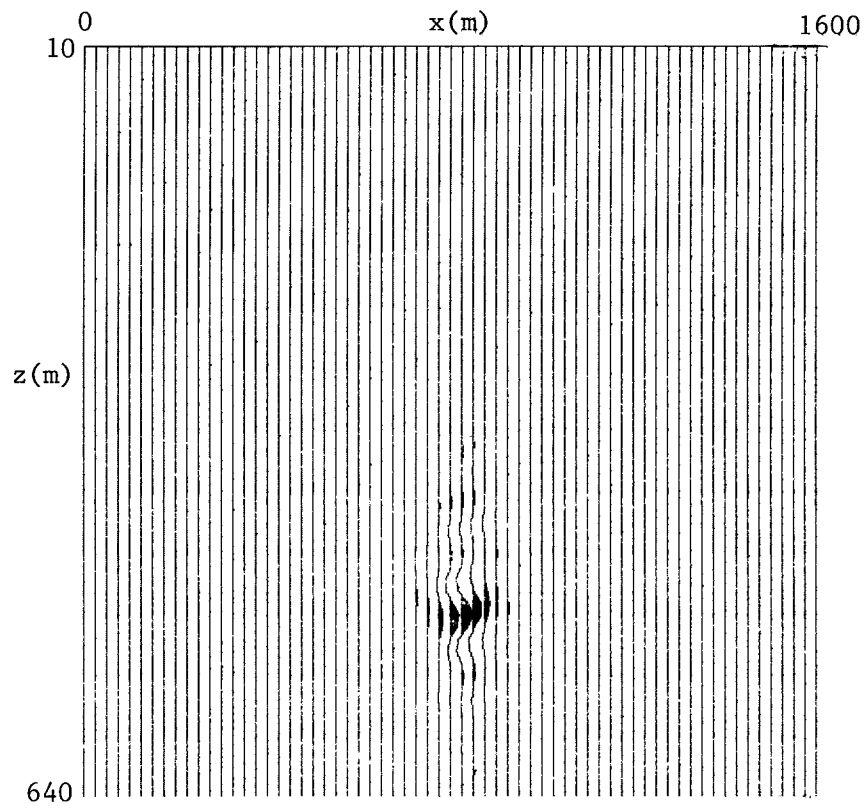
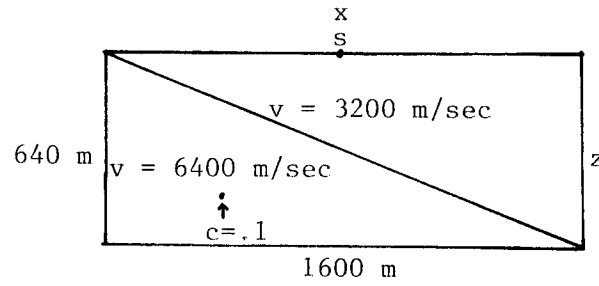
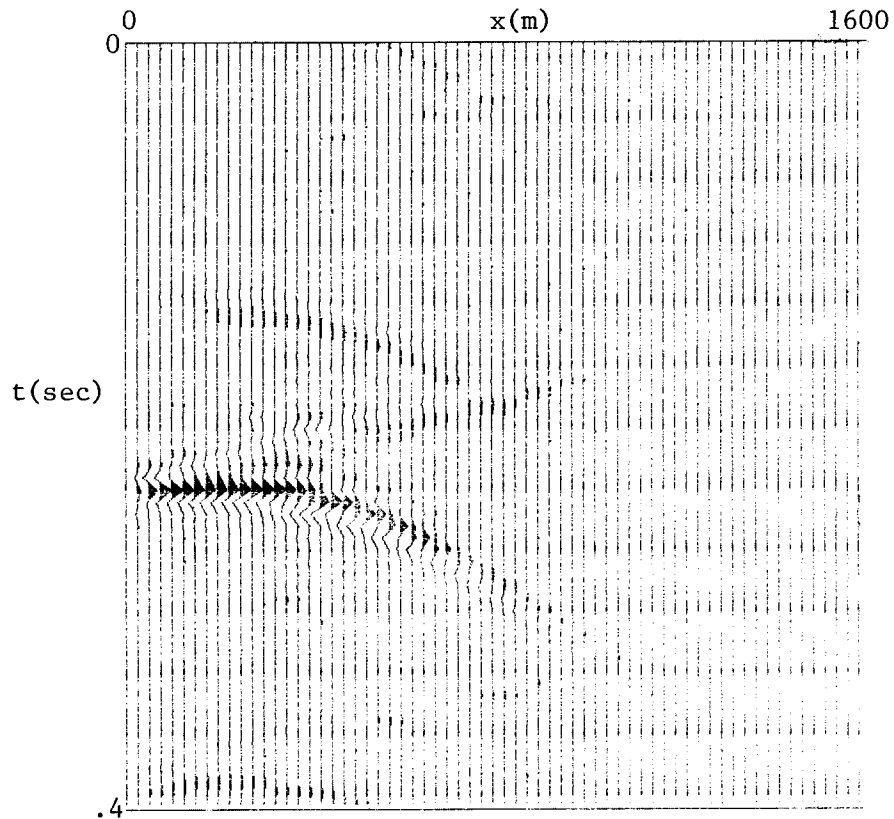


FIGURE 11.--Inversion of Figure 10(b) using  $\sum_{\omega} UD^*$ .



(a)



(b)

FIGURE 12.--(a) Model. Note that the point diffractor is nearly at a  $45^\circ$  angle from the shot, which is not an easy geometry to image with lateral velocity variation. (b) CSG produced from (a).

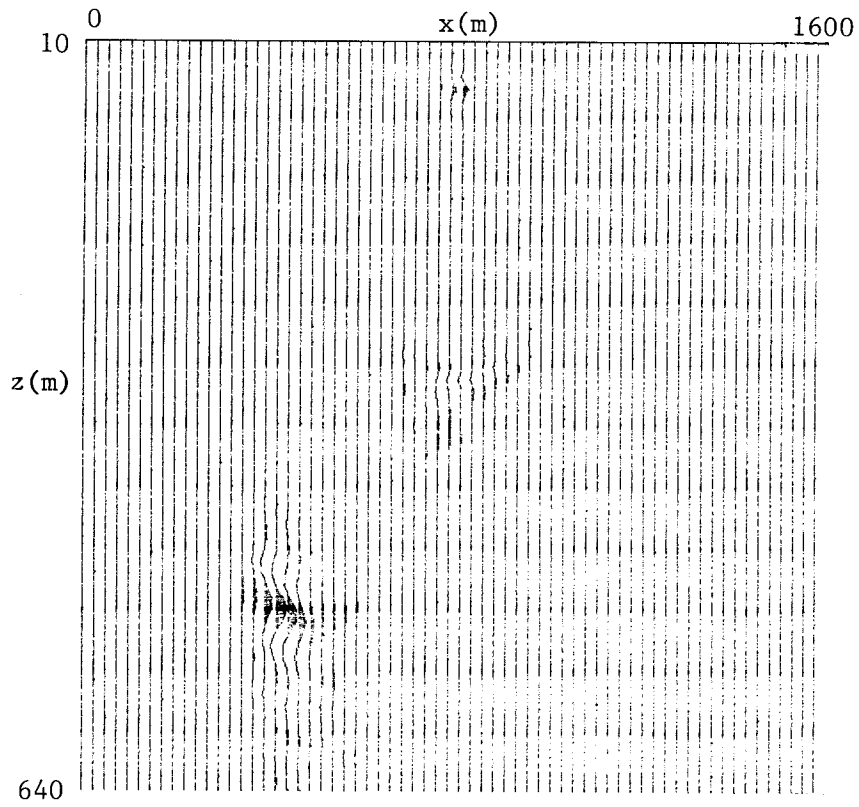


FIGURE 13.--Inversion of Figure 12(b) using  $\sum_{\omega} UD^*$ .

first free surface multiple, and then we repeat this process to produce free surface multiples of any order. This only works for free surface multiples, but they are often the most important anyway when compared to interbed multiples, which we neglect. The CSG can then be compared to the actual data in order to identify the multiples, which can then be zeroed out.

We can also use CSG inversion in conjunction with Don Riley's multiples inversion scheme (SEP-3) in order to remove the multiples while doing a CSG inversion. He works with the  $15^\circ$  equation and constant velocity, but this could easily be extended to the  $45^\circ$  equation and lateral velocity variation. Riley's method must be implemented in the time domain, but Kjartansson's frequency domain method could still be used for downward continuation, and then the waves could be put into the time domain for any particular time  $t$  using  $f(t) = \sum_{\omega} e^{i\omega t} F(\omega)$  for subsequent comparison of  $U$  and  $D$  to remove the multiples. A time domain version of Kjartansson's program could be used, too. There are problems with this approach, however. The multiples must be modeled very accurately in order to remove them with this scheme, and hence shot waveform and velocity errors are even more critical here than with inversion alone.

This same method could also be used for stratified media, however, using the phase shift method for downward continuation, which is exact and much faster than a finite difference scheme. Since we can estimate velocity very accurately with stratified media, this might be a very practical multiples suppression scheme.

Finally, the slant stacking technique described on page        could be used with either the phase shift method or the  $45^\circ$  equation scheme described above to remove multiples.

## REFERENCES

- CLAERBOUT, J.F. (1971), "Toward a unified theory of reflector mapping," *Geophysics* 36:3.
- CLAERBOUT, J.F. (1976), *Fundamentals of Geophysical Data Processing* (New York: McGraw-Hill).
- GAZDAG, J. (1978), "Wave equation migration with the phase shift method," *Geophysics* 43:7.
- JUDSON, D.R., P.S. SCHULTZ and J.W.C. SHERWOOD (1978), "Equalizing the stacking velocities of dipping events via Devilish," presented at the 48th Annual International SEG Meeting, San Francisco, October 31, 1978.
- OTTOLINI, R. (1978), "Migration with slant-midpoint stacks," presented at the 48th Annual International SEG Meeting, San Francisco, October 31, 1978.
- PETERSON, R.A. and W.C. WALTER (1977), *Seismic Imaging Atlas*, Vol. II, United Geophysical Corporation.
- STOLT, R.H. (1978), "Migration by Fourier Transform," *Geophysics* 43:1.